

# The light scalar mesons within quark models

Eef van Beveren <sup>a</sup>, George Rupp <sup>b</sup>,  
 Nicholas Petropoulos <sup>a</sup> and Frieder Kleefeld <sup>b</sup>

<sup>a</sup> *Centro de Física Teórica, Departamento de Física,  
 Universidade, P3004-516 Coimbra, Portugal,  
 (eef@teor.fis.uc.pt and nicholas@teor.fis.uc.pt)*

<sup>b</sup> *Centro de Física das Interacções Fundamentais, Instituto Superior Técnico,  
 Edifício Ciência, P1049-001 Lisboa Codex, Portugal,  
 (george@ajax.ist.utl.pt and kleefeld@cifif.ist.utl.pt)*

Contribution to the  
**Second International Workshop on Hadron Physics,  
 Effective Theories of Low Energy QCD**

at the

Centro de Física Teórica da Universidade de Coimbra 25-29 September, 2002

November 7, 2018

## Abstract

Low-energy meson-meson scattering data are a powerful testing ground for quark models. Here, we describe the behaviour at threshold of  $S$ -wave scattering-matrix singularities.

The majority of the full scattering-matrix mesonic poles stem from an underlying confinement spectrum. However, the light scalar mesons  $K_0^*(830)$ ,  $a_0(980)$ ,  $f_0(400-1200)$ , and  $f_0(980)$  do not, but instead originate in  ${}^3P_0$ -barrier semi-bound states. We show that the behaviour of the corresponding poles is identical at threshold.

In passing, the light-meson sector is given a firm basis.

**Introduction.** It is generally understood that, once the meson sector of strong interactions is fully and consistently described, not too many complications are expected upon including the baryons as well. However, as things stand, important steps have yet to be taken towards a simple quantitative theory for the description of mesons and their interactions [1]. Preferably, this should be a one-parameter theory which, in the limit of free quarks and gluons and some non-abelian interaction, approaches QCD. Here, we pay attention to the unification of all flavours.

For a lowest-order approximation of strong interactions, confinement models may be constructed. Their usefulness can be measured by the models' achievements when adjusting their parameters to experiment[2]. Observed spectra may be interpreted in terms of quark-antiquark or more complicated systems [3]. But in a full theory with quarks and mesons, one can study strong interactions through meson-meson scattering. Consequently, one needs more than confinement only. For further refinements of strong-interaction models, one should compare the models' predictions directly to experimental scattering cross sections and phase shifts when available [4, 5, 6, 7, 8, 9, 10, 11].

Here we will discuss the eternally disputed [12, 13] low-lying nonet of  $S$ -wave poles in meson-meson scattering cross sections, within a four-parameter model [7]. It should thereby be noted that the model's parameters are fitted to the  $J^P = 1^-$   $c\bar{c}$  and  $b\bar{b}$  spectra, as well as to  $P$ -wave meson-meson scattering data [6].

First, let us outline the motivation for our work. For the interaction in the vicinity of a resonance in meson-meson scattering, one may consider quark-exchange or quark-pair-creation processes, giving rise to an intermediate  $q\bar{q}$  system. When the intermediate  $q\bar{q}$  system is close enough to a genuine bound state of confinement, then the system will resonate, resulting in a resonance in meson-meson scattering. Another picture for the same phenomenon is to consider self-energy contributions from virtual meson loops. Either picture describes the same physical situation, namely a mesonic resonance or bound state [14], but in a rather different way. Our aim is to merge both pictures in one model.

**Flavour-independent confinement.** Let us assume that the spectrum of mesonic quark-antiquark systems can be described by flavour-independent harmonic-oscillator confinement. Then, for each pair of flavours, an infinite set of mesons exists with all possible spin, angular, and radial excitations. But, unfortunately, for most flavour pairs only a few angular and even fewer radial recurrences are known [15]. When we do not distinguish up and down, but just refer to non-strange ( $n$ ) quarks and, moreover, ignore the existence of top quarks, then we dispose of four different flavours:  $n$ ,  $s$ ,  $c$ , and  $b$ . These can be combined into ten different flavour pairs, each of which may come in two different spin states: 0 or 1. This gives rise to, in principle, twenty different meson spectra. With some 150 known mesons, this means 7.5 angular plus radial excitations on average, per flavour pair. This is much less than e.g. the known excitations of the positronium spectrum. No wonder that it requires some imagination to guess economic strategies for the description of mesons.

As one may verify from the latest Review of Particle Physics [15], vector states are more numerous than any other type of mesonic resonances, hence better known. Consequently, in order to structure a model we begin with the vector mesons, carrying quantum numbers  $J^P = 1^-$ . In figure (1) we compare the measured  $n\bar{n}$ ,  $c\bar{c}$ , and  $b\bar{b}$  vector states with the possible states of the harmonic oscillator. Most of the data are taken from Ref. [15]. The  $\rho(1290)$  signal has been reported in Refs. [16, 17, 18, 19, 20]. The  $\Upsilon(1D)$  is our interpretation of the  $D$  state which has been observed in Ref. [21].

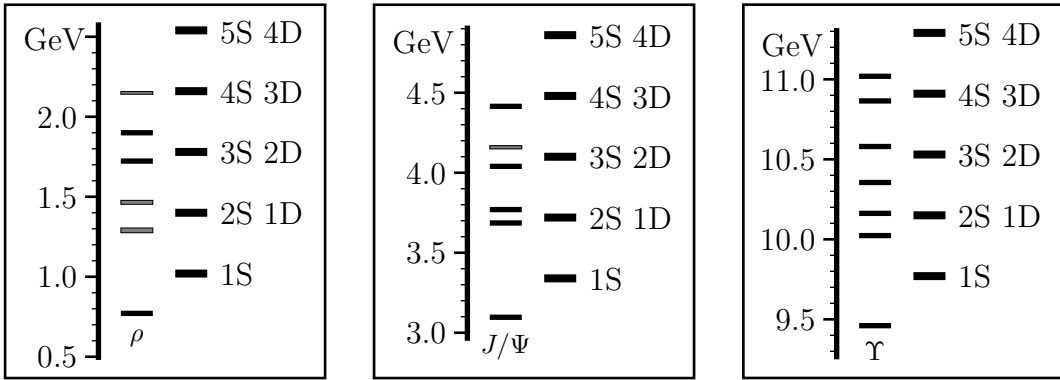


Figure 1: Non-strange, charmonium, and bottomonium  $J^{PC} = 1^{--}$  states compared to the corresponding states from a harmonic-oscillator spectrum. The level spacing for the oscillator equals 0.38 GeV.

The charmonium vector states, shown in figure (1), bear many similarities with the two-particle harmonic oscillator: a ground state in  $S$  wave, and higher radial excitations that are *almost* degenerate with the  $D$ -wave states. Also, except for the ground state, the level spacings are roughly equal. In Ref. [22] the mechanism is discussed which turns the oscillator spectrum into the charmonium spectrum.

For the  $\rho$  and  $\Upsilon$  vector states, also shown in figure (1), we see a very similar pattern: the  $S$ - $D$  splittings are slightly larger, while the  $\rho(770)$  ground state of the  $\rho$  spectrum and the  $\Upsilon(1S)$  ground state of the  $\Upsilon$  spectrum also come out far below the corresponding oscillator ground states. From figure (1) one may moreover conclude that there is not much reason to separate the light-quark sector from the heavy quarks. Below, we discuss the mechanism which turns the oscillator states into the  $\rho$  and  $\Upsilon$  resonances [6].

What we learn from the above comparison is that confinement is flavour independent. Hence, confinement should be described by flavour-independent dynamics. A non-relativistic Schrödinger equation with flavour-mass-dependent harmonic-oscillator [6] is just a perfect example of such dynamics. It casts quark confinement in the form of a one-parameter model. This parameter is the oscillator frequency  $\omega$ , which comes out at about 0.19 GeV for the data.

**Mechanism for more structure.** At this point we dispose of a beautiful one-parameter model for mesons, which has a particularly simple spectrum for each of the flavour and spin excitations, given by

$$M(f, \bar{f}; \ell, n) = \omega \left( 2n + \ell + \frac{3}{2} \right) + m_f + m_{\bar{f}} . \quad (1)$$

Here,  $f$  and  $\bar{f}$  represent the flavours of respectively the quark and the antiquark,  $m_f$  and  $m_{\bar{f}}$  their respective masses,  $\ell$  and  $n$  their relative angular momentum and radial excitation.

Let us study some details of formula (1) in the following. The vector-meson states have unit total angular momentum,  $J = 1$ , and unit  $q\bar{q}$  total spin,  $s = 1$ . Hence, since the parity of vector-meson states equals  $P = -1$ , their orbital angular momentum can be  $\ell = 0$  ( $S$  wave) or  $\ell = 2$  ( $D$  wave). From formula (1) we then understand that, within harmonic-oscillator confinement, the vector-meson states with  $(n, \ell = 2)$  are degenerate with the

vector-meson states with  $(n + 1, \ell = 0)$ , as shown in figure (1). For other flavour and spin excitations similar results emerge. One obtains a very regular, equally spaced spectrum of quark-antiquark states. However, by comparing the experimental meson spectrum to the theoretical harmonic oscillator spectrum (1), we readily see that our simple model by far does not agree with the data.

In order to cure this disagreement, we may study other potentials, which generate spectra that agree better with the data, and even modify, whenever necessary, their parameters for different flavour sectors. But here we prefer to stick to our one-parameter model for all flavours.

When we ignore the electroweak interactions, then the mesons of our model are permanently stable quark-antiquark systems. For the great majority of mesons, this picture badly conflicts with observation. Strong interactions are not just confinement, but also hadronic decay, and elastic and inelastic scattering of hadrons. Our one-parameter model just describes confinement. All other strong phenomena must still be included.

Hadronic decay is quantitatively well described by the phenomenon of quark-pair creation [23], i.e., the creation of a valence quark and a valence antiquark out of the vacuum. Quark pairs are supposed to be created and annihilated all the time inside the realm of a hadron. Only once in a while such pair develops into a valence quark pair, which allows the hadron to decay into other hadrons. We will represent the probability for that process to occur by one parameter,  $\lambda$ , which, in the spirit of flavour symmetry, we assume to be constant for all flavours. In practice, we only consider the creation of non-strange and strange valence quark pairs, since the thresholds for charm and bottom are much higher [24], far above the few mesonic resonances which we want to describe.

Both  $\lambda$  and the oscillator frequency  $\omega$  should be related to the fundamental parameter  $\alpha$  of QCD. However, having no knowledge about such relation, we accept them as free parameters. Nevertheless, they are chosen independent of the flavour pair which constitutes the meson under consideration. This way we guarantee flavour independence of our model's results, as dictated by QCD, and reconfirmed by experiment [25].

We suppose that quark-pair creation takes place in the interior of a hadron, neither at very large (confinement), nor at very small (asymptotic freedom) interquark distances. In the coordinate representation, these considerations get translated into a potential  $V_t$  of the form as depicted in figure (2). This transition potential enables the communication between a meson and its decay products.

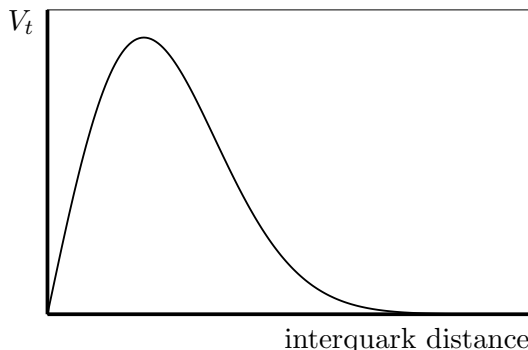


Figure 2: Form of the transition potential  $V_t$  in the coordinate representation

The principle of flavour independence of strong interactions demands that the transition potential cannot be a function of the pure interquark distance  $r$ , but has to be scaled by the reduced mass  $\mu$  of the flavours of the system, *i.e.*

$$V_t = V_t(\sqrt{\mu} r) . \quad (2)$$

The model's results are then to lowest order flavour independent. Differences, which also can be observed in the data, stem from the higher orders and kinematics.

We have chosen the form of  $V_t$  such that it depends on two, again flavour-independent, parameters. This completes the description of the model, which, besides the four constituent quark masses, has four model parameters.

**Non-exotic meson-meson scattering.** The model under discussion is taylor-made for describing non-exotic meson-meson scattering. In particular, for processes of the form

$$\text{meson } A + \text{meson } B \longrightarrow q\bar{q} \longrightarrow \text{meson } C + \text{meson } D , \quad (3)$$

where it is understood that all flavours are such that the  $q\bar{q}$  system couples to the  $AB$  two-meson system by light-quark-pair annihilation and to the  $CD$  two-meson system by light-quark-pair creation. Processes with more than two mesons in the final state are supposed to come from subsequent decays of the mesons in the initial  $CD$  two-meson final state, and hence to be of less importance for the properties we want to study.

In the interaction region, where our model applies, we have a finite probability to find an  $AB$  two-meson system, or a  $CD$  two-meson system, or a  $q\bar{q}$  mesonic system. The latter is usually far from its confinement eigenstates and thus highly unstable. The  $CD$  pair represents any of the unlimited number of possible two-meson final states. In Ref. [26] it is described how the two-meson final states can be limited to a finite number of possibilities. Additionally, we only take the lowest-lying pseudoscalar,  $\pi$ ,  $K$ ,  $\eta$ , or  $\eta'$ , and vector mesons  $\rho$ ,  $K^*$ ,  $\omega$ , or  $\phi$ , as final-state particles. Nevertheless, the number of final-state channels comes out mostly somewhere between ten and twenty. However, in Ref. [27] it is shown that, when one takes relatively small errors of up to some 50 MeV for granted, then one may even obtain part of the results for low energies by just including the lowest-lying, or the most important, final-state channel.

The above-discussed parameter  $\lambda$  represents the overall three-meson-vertex coupling of the two-meson channels to the  $q\bar{q}$  channel of expression (3). Relative couplings for the various three-meson vertices that may occur can be determined by a technique described in Ref. [26]. In some cases one also has various possible  $q\bar{q}$  channels, as the isosinglets,  $n\bar{n}$ ,  $s\bar{s}$ , ... mix with one another.

The probability to find a certain two-particle state in the interaction region can be determined from its wave function. Consequently, the model can be formulated in terms of a multichannel system of coupled-channel equations for the various wave functions. Details may be found in Ref. [6]. By a technique which has been described in Ref. [28], one can analytically solve the coupled-channel equations and determine the scattering matrix  $S(\sqrt{s})$  as a function of the total centre-of-mass energy. Subsequently one may study elastic cross sections, or phase shifts, but also inelasticities and wave functions. Moreover, the solutions of the coupled-channel equations may be analytically continued to complex values of  $\sqrt{s}$ , which allows to study the pole structure of the scattering matrix in the complex-energy plane.

**Bound states and resonances.** Each of the two-meson final-state channels has a minimum value for the energy at which the two mesons can be formed, the threshold energy, which is given by the sum of the two meson masses. When the total energy  $\sqrt{s}$  of the coupled-channel system is above the threshold of a particular channel, one says that the channel is open. It means that scattering is possible for that channel. Nevertheless, it is legitimate to study the solutions of the set of coupled-channel equations for energies below the thresholds, i.e., when channels are closed. In particular, below the lowest threshold, where all channels are closed and no scattering is possible, one may obtain the analytic continuation in  $\sqrt{s}$  of the scattering matrix.

Singularities in  $S(\sqrt{s})$  for real values of  $\sqrt{s}$  below the lowest threshold, represent permanently bound states, when calculated in the correct Riemann sheet (i.e., with positive imaginary momenta  $k$  in all channels). The wave functions corresponding to those singularities have for all channels contributions that rapidly vanish at large interparticle distances. They represent the stable mesons, like the  $J/\Psi$ , which cannot decay strongly. For ground states of pseudoscalar and vector mesons, one finds the poles shifted to mass values which are far below the corresponding oscillator ground states. The sizes of the shifts are roughly proportional to  $\lambda^2$ , and may have values of several hundreds of MeV. The higher excitations of pseudoscalar and vector mesons shift much less. For this reason, one may start from harmonic-oscillator confinement and yet end up with realistic meson spectra [22]. We achieve this for all mesons with one fixed value for each of the four model parameters [6].

The fact that all channels contribute to the wave function of stable mesons implies that stable mesons, too, have two-meson components, not just  $q\bar{q}$ . This observation has important consequences for electromagnetic and weak transitions of stable mesons [29].

Above the lowest threshold no bound states can exist. Accordingly, one does not find singularities in the scattering matrix on the real  $\sqrt{s}$  axis. The poles which are found in that region of the complex  $\sqrt{s}$  plane have real and imaginary parts. When a pole is encountered in the lower half of the complex  $\sqrt{s}$  plane, and moreover in the right Riemann sheet and not too far from the real axis, then one may observe a nearby enhancement in the elastic cross sections of all open channels. These structures represent the resonances that show up in meson-meson scattering, as e.g. the  $\rho$  meson in  $\pi\pi$  scattering, and the  $K^*$  meson in  $K\pi$  scattering.

In the quark-exchange picture, we obtain a resonance in the particular partial-wave meson-meson-scattering cross section which matches the quantum numbers of the intermediate  $q\bar{q}$  system of process (3). Such a phenomenon may be described by scattering phase shifts of the Breit-Wigner [30] form

$$\cotg(\delta_\ell(s)) \approx \frac{E_R - \sqrt{s}}{\Gamma_R/2} \quad , \quad (4)$$

where  $E_R$  and  $\Gamma_R$  represent the central invariant meson-meson mass and the resonance width, respectively.

However, formula (4) is a good approximation for the scattering cross section only when the resonance shape is not very much distorted and the width of the resonance is small. Moreover, the intermediate state in such a process is essentially a constituent  $q\bar{q}$  configuration that is part of a confinement spectrum (also referred to as bare or intrinsic state), and hence may resonate in one of the eigenstates. This implies that the colliding mesons scatter off the whole  $q\bar{q}$  confinement spectrum of radial, and possibly also angular excitations, not just off one single state [31]. Consequently, a full expression for the phase

shifts of formula (4) should contain all possible eigenstates of such a spectrum as long as quantum numbers are respected. Let us denote the eigenvalues of the relevant part of the spectrum by  $E_n$  ( $n = 0, 1, 2, \dots$ ), and the corresponding eigenstates by  $\mathcal{F}_n$ . Then, following the procedure outlined in Ref. [27], we may write for the partial-wave phase shifts the more general expression

$$\cotg(\delta(s)) = \left[ I(s) \sum_{n=0}^{\infty} \frac{|\mathcal{F}_n|^2}{\sqrt{s} - E_n} \right]^{-1} \left[ R(s) \sum_{n=0}^{\infty} \frac{|\mathcal{F}_n|^2}{\sqrt{s} - E_n} - 1 \right] . \quad (5)$$

In  $R(s)$  and  $I(s)$  we have absorbed the kinematical factors and details of two-meson scattering, and moreover the three-meson vertices. The details of formula (5) can be found in Ref. [27].

For an approximate description of a specific resonance, and in the rather hypothetical case that the three-meson vertices have small coupling constants, one may single out, from the sum over all confinement states, one particular state (say number  $N$ ), the eigenvalue of which is nearest to the invariant meson-meson mass close to the resonance. Then, for total invariant meson-meson masses  $\sqrt{s}$  in the vicinity of  $E_N$ , one finds the approximation

$$\cotg(\delta(s)) \approx \frac{[E_N + R(s) |\mathcal{F}_N|^2] - \sqrt{s}}{I(s) |\mathcal{F}_N|^2} . \quad (6)$$

Formula (6) is indeed of the form (4), with the central resonance position and width given by

$$E_R \approx E_N + R(s) |\mathcal{F}_N|^2 \quad \text{and} \quad \Gamma_R \approx 2I(s) |\mathcal{F}_N|^2 . \quad (7)$$

In experiment one observes the influence of the nearest bound state of the confinement spectrum, as in classical resonating systems. Nevertheless, formula (6) is only a good approximation when the three-meson couplings are small. Since the coupling of the meson-meson system to quark exchange is strong, the influence of the higher- and lower-lying excitations is not negligible.

In data analyses one usually represents a resonance in the elastic cross section by a Breit-Wigner structure, associated with a singularity in the complex  $\sqrt{s}$  plane. In our model resonances are not well represented by Breit-Wigner structures, due to non-perturbative effects. A good example is the  $\rho'(1250)$ . This resonance is omitted from the meson tables of the Review of Particle Physics. Nevertheless, it is reported in data analyses as a clear signal [16, 17, 20]. In our model it comes out as a very tiny structure around 1.26 GeV in coupled  $\pi\pi$ ,  $K\bar{K}$ ,  $\eta_n\rho$ ,  $\pi\omega$ ,  $KK^*$ ,  $\rho\rho$ ,  $K^*K^*$  scattering in the tail of the  $\rho(770)$  resonance [6]. Now, since in the data analyses quoted in [15] one uses Breit-Wigner structures, it is no surprise that for this tiny effect, which moreover has a rather large width, no evidence is found. At the position of the  $\rho'(1470)$ , which in Ref. [15] is claimed to be the first radial  $\rho$  excitation, we find a  $D$  resonance, which has the same quantum numbers as the  $S$  state. Naturally, we may know which resonance is dominantly  $S$  and which is dominantly  $D$ , since we can determine the wave functions in our model. From cross sections alone one cannot easily distinguish [32] between the two.

In the other hypothetical limit, namely of very large couplings, we obtain for the phase shift the expression

$$\cotg(\delta(s)) \approx \frac{R(s)}{I(s)} , \quad (8)$$

which describes scattering off an infinitely hard cavity.

The physical values of the couplings come out somewhere in between the two hypothetical cases. Most resonances and bound states can be classified as stemming from a specific confinement state [33, 34]. However, some structures in the scattering cross section stem from the cavity which is formed by quark exchange or pair creation [27]. The most notable of such states are the low-lying resonances observed in *S*-wave pseudoscalar-pseudoscalar scattering [35, 36, 37, 38].

From the above discussion one may conclude that, to lowest order, the mass of a meson follows from the quark-antiquark confinement spectrum. It is, however, well-known that higher-order contributions to the meson propagator, in particular those from meson loops, cannot be neglected. Virtual meson loops give a correction to the meson mass, whereas decay channels also contribute to the strong width of the meson. One obtains for the propagator of a meson the form

$$\Pi(s) = \frac{1}{s - (M_{\text{confinement}} + \sum \Delta M_{\text{meson loops}})^2} , \quad (9)$$

where  $\Delta M$  develops complex values when open decay channels are involved.

For the full mass of a meson, all possible meson-meson loops have to be considered. A model for meson-meson scattering must therefore include all possible inelastic channels as well. Although in principle this could be done, in practice it is not feasible, unless a scheme exists dealing with all vertices and their relative intensities. In Ref. [26] relative couplings have been determined in the harmonic-oscillator approximation, assuming  $^3P_0$  quark exchange. However, further kinematical factors must be worked out and included.

In its present form, the model is far from perfect. However, it allows for many predictions and for a good classification of the mesonic resonances. It moreover serves well as an interface between QCD quenched-lattice calculations and experiment. Quenched calculations describe confinement. As we have shown, the confinement spectrum and wave functions are very different from the hadronic reality for mesons. Applying the model, we may indicate what differences must be anticipated. For example, on the lattice one finds the lowest scalar-meson states at 1.3–1.5 GeV, exactly as we find for the pure harmonic oscillator. But the model yields a further nonet of scalar resonances well below 1.0 GeV. Hence, it is neither a failure of lattice QCD, nor of experiment! The light scalar resonances just do not form part of the confinement spectrum.

**The spectrum.** The complete model consists of an expression for the  $K$  matrix, similar to formula (5), but extended to many meson-meson scattering channels, several constituent quark-antiquark channels, and more complicated transition potentials [6, 7], which at the same time and with the same set of four parameters reproduces bound states, partial-wave scattering quantities, and the electromagnetic transitions of  $c\bar{c}$  and  $b\bar{b}$  systems [29].

The  $K$  matrix can be analytically continued below the various thresholds, even the lowest one, with no need of redefining any of the functions involved, in order to study the singularities of the corresponding scattering matrix. Below the lowest threshold, these poles show up on the real  $\sqrt{s}$  axis, and can be interpreted as the bound states of the coupled system, to be identified with the stable mesons. For the light flavours one finds this way a

nonet of light pseudoscalars, i.e., the pion, Kaon, eta, and eta'. For the heavy flavours, the lowest-lying model poles can be identified with the  $D(1870)$ ,  $D_s(1970)$ ,  $\eta_c(1S)$ ,  $J/\psi(1S)$ ,  $\psi(3686)$ ,  $B(5280)$ ,  $B_s(5380)$ ,  $\Upsilon(1S)$ ,  $\Upsilon(2S)$ , and  $\Upsilon(3S)$ .

Above the lowest threshold, the model's partial-wave cross sections and phase shifts for all included meson-meson channels can be calculated and compared to experiment, as well as the inelastic transitions. Out of the many singularities of the scattering matrix in a rather complex set of Riemann sheets, some come out with negative imaginary part in the  $\sqrt{s}$  plane, and moreover close enough to the physical real axis so as to be noticed in the partial-wave phase shifts and cross sections. These can be identified with the known resonances, like the  $\rho$  pole in  $\pi\pi$  scattering, or the  $K^*$  pole in  $K\pi$  scattering. However, there may always be a pole in a nearby Riemann sheet just around the corner of one of the thresholds, which can be noticed in the partial-wave cross section. The study of poles is an interesting subject by itself [39, 40].

**Scattering-matrix poles.** In the hypothetical case of very small couplings for the three-meson vertices, we obtain poles in the scattering matrix that are close to the eigenvalues of the confinement spectrum. Let us denote by  $M_1$  and  $M_2$  the meson masses, and by  $\Delta E$  the difference between the complex-energy pole of the scattering matrix and the energy eigenvalue,  $E_N$ , of the nearby state of the confinement spectrum. Using formula (7), we obtain

$$\Delta E \approx \{R(s) - iI(s)\} |\mathcal{F}_N|^2 . \quad (10)$$

We may distinguish two different cases:

- (1)  $E_N > M_1 + M_2$  (above threshold),
- (2)  $E_N < M_1 + M_2$  (below threshold).

When the nearby state of the confinement spectrum is in the scattering continuum, then  $\Delta E$  has a **negative** imaginary part and a real part, since both  $R(s)$  and  $I(s)$  of formula (10) are real, and  $I(s)$  is moreover positive. The resonance singularity of the scattering matrix is in the lower half of the complex-energy plane (second Riemann sheet), as is depicted on the right-hand side of threshold in Fig. (3).

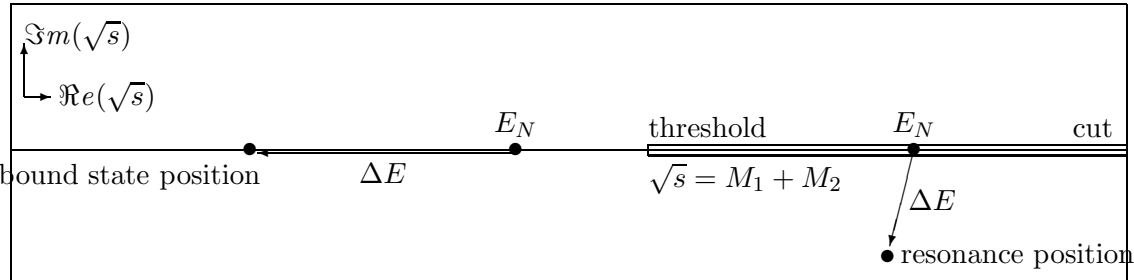


Figure 3: When the confinement state on the real  $\sqrt{s}$  axis is below the lowest scattering threshold, then the bound-state singularity comes out on the real  $\sqrt{s}$  axis. On the other hand, when the confinement state on the real  $\sqrt{s}$  axis is in the scattering continuum, then for small coupling (perturbative regime) the resonance pole moves into the lower half of the complex  $\sqrt{s}$  plane.

When the nearby state of the confinement spectrum is below the scattering threshold,

then  $\Delta E$  has only a real part, since  $I(s)$  turns purely imaginary below threshold, whereas  $R(s)$  remains real. The bound-state singularity of the scattering matrix corresponding to this situation remains on the real axis of the complex-energy plane, as is depicted on the left-hand side of threshold in Fig. (3).

**Threshold behaviour.** Near the lowest threshold, as a function of the overall coupling constant,  $S$ -wave poles behave very differently from  $P$ - and higher-wave poles. This can easily be understood from the effective-range expansion [41] at the pole position. There, the cotangent of the phase shift equals  $i$ . Hence, for  $S$  waves the next-to-lowest-order term in the expansion equals  $ik$  ( $k$  represents the linear momentum related to  $s$  and the lowest threshold). For higher waves, on the other hand, the next-to-lowest-order term in the effective-range expansion is proportional to  $k^2$ .

Poles for  $P$  and higher waves behave in the complex  $k$  plane as indicated in Fig. (4b). The two  $k$ -plane poles meet at threshold ( $k = 0$ ). When the coupling constant of the model is increased, the poles move along the imaginary  $k$  axis. One pole moves towards negative imaginary  $k$ , corresponding to a virtual bound state below threshold on the real  $\sqrt{s}$  axis, but in the wrong Riemann sheet. The other pole moves towards positive imaginary  $k$ , corresponding to a real bound state.

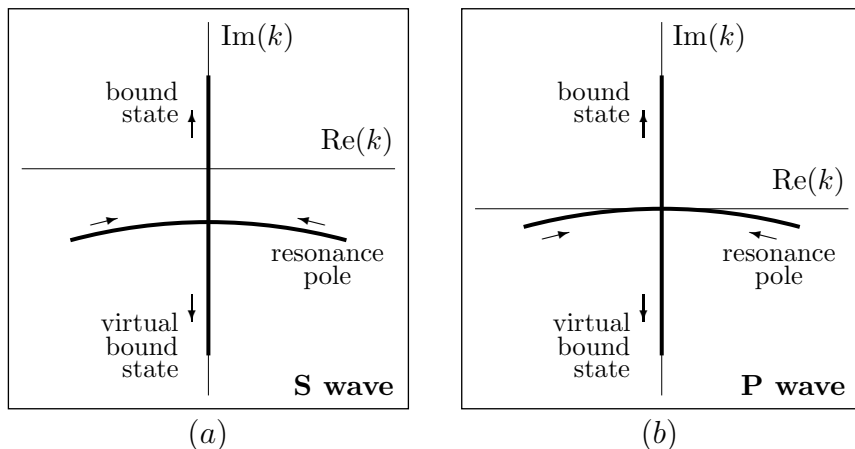


Figure 4: Variation of the positions of scattering-matrix poles as a function of hypothetical variations in the three-meson-vertex coupling, for  $S$  waves (a), and for  $P$  and higher waves (b). The arrows indicate increasing coupling constant.

For  $S$ -wave poles, the behaviour is shown in Fig. (4a). The two  $k$ -plane poles meet on the negative imaginary  $k$  axis. When the coupling constant of the model is slightly increased, both poles continue on the negative imaginary  $k$  axis, corresponding to two virtual bound states below threshold on the real  $\sqrt{s}$  axis. Upon further increasing the coupling constant of the model, one pole moves towards increasing negative imaginary  $k$ , thereby remaining a virtual bound state for all values of the coupling constant. The other pole moves towards positive imaginary  $k$ , eventually crossing threshold ( $k = 0$ ), thereby turning into a real bound state of the system of coupled meson-meson scattering channels. Hence, for a small range of hypothetical values of the coupling constant, there are two virtual bound states, one of which is very close to threshold. Such a pole certainly has a noticeable influence on the scattering cross section.

**The low-lying nonet of S-wave poles.** The nonet of low-lying S-wave poles behave as described above, with respect to variations of the model's overall coupling constant. However, they do not stem from the confinement spectrum, but rather from the cavity. For small values of the coupling, such poles disappear into the continuum, i.e., they move towards negative imaginary infinity [27], and not towards an eigenstate of the confinement spectrum as in Fig. (3).

In Fig. (5) we study the hypothetical pole positions of the  $K_0^*(730)$  pole in  $K\pi$  S-wave scattering. The physical value of the coupling constant equals 0.75, which is not shown in Fig. (5). A figure for smaller values of the coupling constants can be found in Ref. [27]. The physical pole in  $K\pi$  isodoublet S-wave scattering, related to experiment [37, 36], comes out at  $727 - i263$  MeV in Ref. [7]. Here we concentrate on the threshold behaviour of the hypothetical pole movements in the complex  $k$  and  $\sqrt{s}$  planes. Until they meet on the axis, which is for a value of the coupling constant slightly larger than 1.24, we have only depicted the right-hand branch.

In the left-hand picture of Fig. (5) we observe how the poles arrive on the imaginary  $k$  axis, and then continue to move along that axis. One of the poles moves upwards, initially describing a virtual bound state, and crossing the real  $k$  axis for a value of the coupling constant slightly larger than 1.30. The other pole moves downwards, remaining a virtual bound state for further increasing values of the coupling constant.

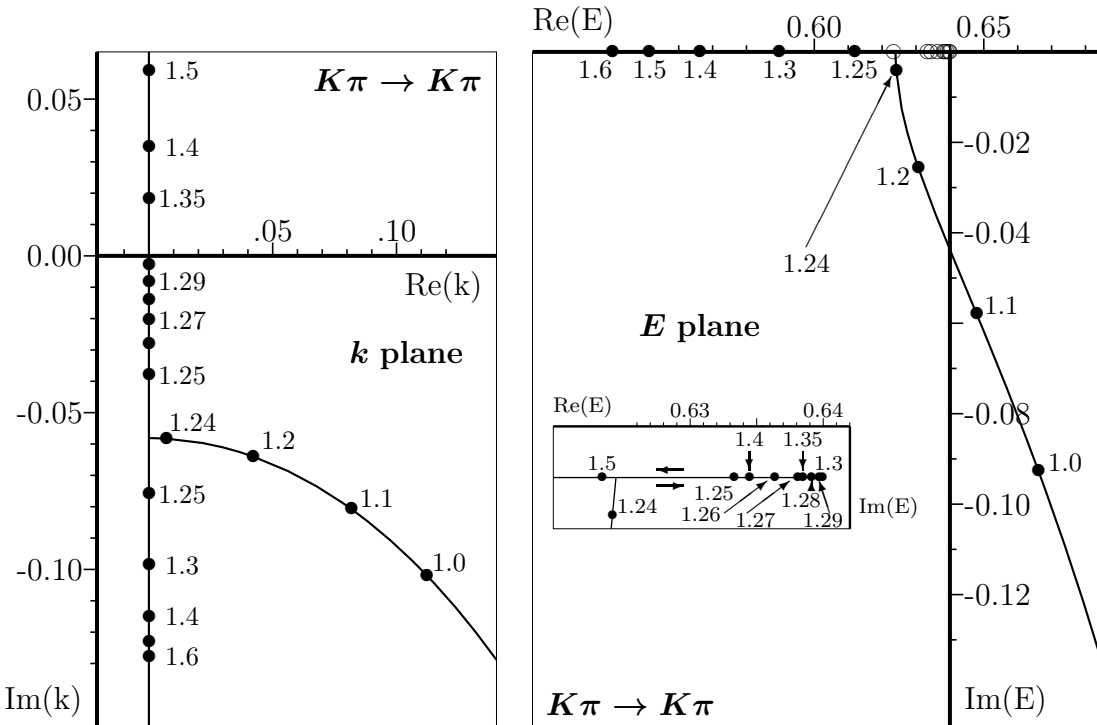


Figure 5: Hypothetical movement of the  $K_0^*(730)$  pole in  $K\pi$  S-wave scattering as a function of the coupling constant. The two branches on the imaginary  $k$  axis are discussed in the text. In the  $E = \sqrt{s}$  plane these two branches come out on the real axis below threshold. The poles of the upper branch are shown as open circles in the main figure, and as closed circles in the inset. Units are in GeVs.

In the right-hand picture of Fig. (5) the same pole has been depicted in the complex  $\sqrt{s}$  plane. Here, the situation is more confusing, since the pole positions are in the same interval of energies. The pole corresponding to the one moving downwards along the imaginary  $k$  axis moves to the left on the real  $\sqrt{s}$  axis. Its positions as a function of the coupling constant are indicated by solid circles. The pole moving upwards along the imaginary  $k$  axis initially moves towards threshold and then turns back, following the former pole, but in a different Riemann sheet. The positions of the latter pole are indicated by open circles. In the inset we try to better clarify its motion. Notice that, since we took 0.14 GeV and 0.50 GeV for the pion and the Kaon mass, respectively, we end up with a threshold at 0.64 GeV.

It is interesting to notice that in a recent work of Boglione and Pennington [42] also a zero-width state is found below the  $K\pi$  threshold in  $S$ -wave scattering. Here, we obtain such a state for *unphysical* values of the coupling.

In Fig. (6) we have depicted the movement of the  $a_0(980)$  pole in  $S$  wave  $I = 1$   $KK$  scattering (threshold at 1.0 GeV) on the upwards-going branch. One observes a very similar behaviour as in the case of  $K\pi$  scattering, but with two important differences, to be described next.

The  $K_0^*(730)$  poles meet on the real  $\sqrt{s}$  axis only 16 MeV below threshold (see Fig. 5), and for a value of the coupling constant which is well above the physical value of 0.75, whereas the  $a_0(980)$  poles meet 238 MeV below threshold, when the coupling constant only equals 0.51. At the physical value of the coupling constant, the  $a_0(980)$  pole is a real bound state some 9 MeV below threshold.

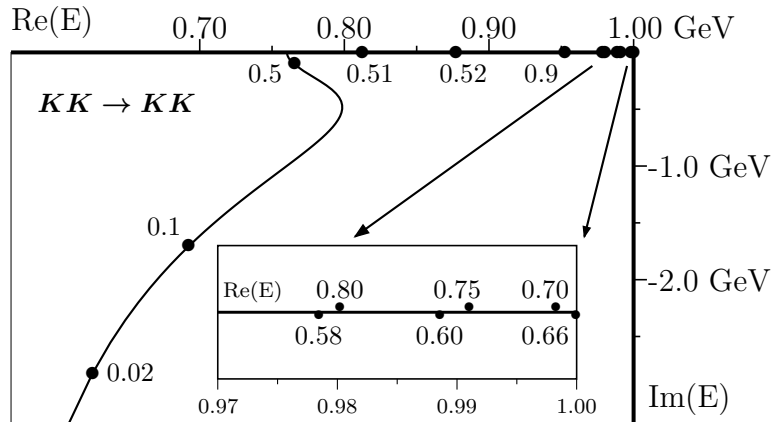


Figure 6: Pole movement as a function of the coupling constant for  $KK$   $I = 1$   $S$ -wave scattering. Some values of the coupling constant are indicated in the figure. The six filled circles at the right end of the real axis correspond, from left to right, to the values 0.58, 0.80, 0.60, 0.75, 0.70, and 0.66 for the model's coupling constant. This situation is magnified in the inset.

But there is yet another difference. Whereas the  $K\pi$  channel represents the lowest possible scattering threshold for the  $K_0^*(730)$  system,  $KK$  is not the lowest channel for the  $a_0(980)$ . In a more complete description, at least all pseudoscalar meson-meson loops should be taken into account. One of these is the  $\eta\pi$  channel, which has a threshold well

below  $KK$ . Consequently, upon including the  $\eta\pi$  channel in the model, the pole cannot remain on the real  $\sqrt{s}$  axis, but has to acquire an imaginary part, in a similar way as shown in Fig. (3). In Ref. [7] we obtained a resonance-like structure in the  $\eta\pi$  cross section, representing the physical  $a_0(980)$ . The corresponding pole came out at  $962 - i28$  MeV.

For the  $f_0(980)$  system the situation is very similar to that of the  $a_0(980)$ . Assuming a pure  $s\bar{s}$  quark content [43], we obtain for the variation of the corresponding pole in  $KK$   $I = 0$   $S$ -wave scattering a picture almost equal to the one shown in Fig. (6). However, only in lowest order the  $KK$  channel could be considered the lowest threshold for the  $f_0(980)$  system. In reality,  $s\bar{s}$  also couples to the non-strange quark-antiquark isosinglet through  $KK$ , and hence to  $\pi\pi$  [8]. This coupling is nevertheless very weak, which implies that the resulting pole does not move far away from the  $KK$  bound state. In Ref. [7] we obtained a resonance-like structure in the  $\pi\pi$  cross section representing the physical  $f_0(980)$ . The corresponding pole came out at  $994 - i20$  MeV.

At lower energies, we found for the same cross section a pole which is the equivalent of the  $K_0^*(730)$  system, but now in  $\pi\pi$  isoscalar  $S$ -wave scattering. This pole at  $470 - i208$  MeV may be associated with the  $\sigma$  meson, since it has the same quantum numbers, and lies in the ballpark of predicted pole positions in models of the  $\sigma$  (for a complete overview of  $\sigma$  poles, see Ref. [22]).

We do not find any other relevant poles in the energy region up to 1.0 GeV.

**Conclusions.** We have shown that the poles of the  $a_0(980)$  and  $f_0(980)$  belong to a nonet of scattering-matrix poles. The lower-lying isoscalar pole and the isodoublet poles in the complex-energy plane have real parts of 0.47 GeV and 0.73 GeV, respectively, and imaginary parts of 0.21 GeV resp. 0.26 GeV. Whether these poles represent real physical resonances [44] is not so relevant here. Important is that the  $a_0(980)$  and  $f_0(980)$  are well classified within a nonet of scattering-matrix poles with very specific characteristics, different from those of the poles stemming from confinement, like the confinement-ground-state nonet of scalar mesons  $f_0(1370)$ ,  $a_0(1450)$ ,  $K_0^*(1430)$ , and  $f_0(1500)$ . The latter poles vary as a function of the coupling constant exactly the way indicated in figure (3). For vanishing coupling constant they end up on the real  $\sqrt{s}$  axis at the positions of the various ground-state eigenvalues of the confinement spectrum, which are the light-flavour  $^3P_0$  states at 1.3 to 1.5 GeV [45, 46].

The low-lying  $S$ -wave poles related to the cross sections in the  $f_0(470)$ ,  $K_0^*(730)$ ,  $f_0(980)$ , and  $a_0(980)$  regions move to negative imaginary infinity in the  $\sqrt{s}$  plane for decreasing values of the coupling. The pole positions for the physical value of the coupling are well explained by their threshold behaviour. Whether or not these poles have large imaginary parts, leading to large widths and strong resonance distortion, depends in a subtle way on the thresholds and couplings of the various relevant scattering channels [47].

As to the nature of the light scalar mesons, which has recently been discussed in Refs. [12, 13, 48, 49], we can only remark that in a many-coupled-channel model each of the channels contributes to the states under the resonance, not just one specific channel.

We have moreover shown that the **principle of flavour independence for the strong interactions** has far-reaching consequences for the construction of hadron models. Applied as a guiding principle for building a largely non-relativistic many-coupled-channel Schrödinger equation for meson-meson scattering, it results in a surprisingly complete model for mesons and mesonic resonances. Its description of the light scalar resonances leaves no doubt on where these mesons are, nor on how to classify them.

**Acknowledgement:** This work has been partly supported by the *Fundaçao para a Ciéncia e a Tecnologia* of the *Ministério da Ciéncia e da Tecnologia* of Portugal, under contract numbers POCTI/35304/FIS/2000, CERN/FIS/43697/2001, PRAXIS XXI/BPD/-20186/99, and SFRH/BPD/9480/2002.

## References

- [1] J. Schechter, eConf **C010815** (2002) 76 [arXiv:hep-ph/0112205].
- [2] S. Godfrey and N. Isgur, Phys. Rev. D **32** (1985) 189.
- [3] J. Vijande, F. Fernández, A. Valcarce, B. Silvestre-Brac, Contributed to Meson 2002: 7th International Workshop on Meson Production, Properties and Interaction, Cracow, Poland, 24-28 May 2002, arXiv:hep-ph/0206263.
- [4] E. Eichten, *In \*Cargese 1975, Proceedings, Weak and Electromagnetic Interactions At High Energies, Part A\**, New York 1976, 305-328.
- [5] E. Eichten, K. Gottfried, T. Kinoshita, K. D. Lane and T. M. Yan, Phys. Rev. D **21** (1980) 203.
- [6] E. van Beveren, G. Rupp, T. A. Rijken, and C. Dullemond, Phys. Rev. **D27** (1983) 1527.
- [7] E. van Beveren, T. A. Rijken, K. Metzger, C. Dullemond, G. Rupp and J. E. Ribeiro, Z. Phys. **C30** (1986) 615.
- [8] R. N. Cahn and P. V. Landshoff, Nucl. Phys. B **266** (1986) 451.
- [9] Nils A. Törnqvist and Matts Roos, Phys. Rev. Lett. **76** (1996) 1575 [arXiv:hep-ph/9511210].
- [10] Frank E. Close, Int. J. Mod. Phys. A **17** (2002) 3239 [arXiv:hep-ph/0110081].
- [11] Agnieszka Furman and Leonard Leśniak, Phys. Lett. B **538** (2002) 266 [arXiv:hep-ph/0203255].
- [12] Frank E. Close and Nils A. Törnqvist, J. Phys. G **28** (2002) R249 [arXiv:hep-ph/0204205].
- [13] Nils A. Törnqvist, arXiv:hep-ph/0201171.
- [14] Frank E. Close and Nathan Isgur, Phys. Lett. B **509** (2001) 81 [arXiv:hep-ph/0102067].
- [15] K. Hagiwara *et al.* [Particle Data Group Collaboration], *Review Of Particle Physics*, Phys. Rev. D **66** (2002) 010001.
- [16] D. Aston *et al.*, SLAC-PUB-5606 (1994).
- [17] D. Aston *et al.*, Nucl. Phys. Proc. Suppl. **21** (1991) 105.
- [18] A. B. Govorkov, JINR-P2-86-682 (1986).

- [19] S. Bartalucci *et al.*, Nuovo Cim. A **49** (1979) 207.
- [20] J. Ballam *et al.*, Nucl. Phys. B **76** (1974) 375.
- [21] S. E. Csorna *et al.* [CLEO Collaboration], arXiv:hep-ex/0207060.
- [22] Eef van Beveren and George Rupp, Proceedings of the Workshop on Recent Developments in Particle and Nuclear Physics, April 30, 2001, Coimbra (Portugal) ISBN 972-95630-3-9, pages 1-16, [arXiv:hep-ph/0201006].
- [23] G. Zweig, CERN Reports TH-401 and TH-412, see also *Developments in the Quark Theory of Hadrons*, Vol. 1\*, 22-101 (1981) editted by D. B. Lichtenberg and S. P. Rosen.
- [24] N. Brambilla, Y. Sumino and A. Vairo, Phys. Rev. D **65** (2002) 034001 [arXiv:hep-ph/0108084].
- [25] K. Abe *et al.* [SLD Collaboration], Phys. Rev. D **59** (1999) 012002 [arXiv:hep-ex/9805023].
- [26] E. van Beveren, Z. Phys. **C21** (1984) 291.
- [27] Eef van Beveren and George Rupp, Eur. Phys. J. **C22**, 493 (2001) [arXiv:hep-ex/0106077].
- [28] E. van Beveren, C. Dullemond, T. A. Rijken, and G. Rupp, Lect. Notes Phys. **211** (1984) 182.
- [29] A. G. Verschuren, C. Dullemond, and E. van Beveren, Phys. Rev. **D44** (1991) 2803.
- [30] G. Breit and E. Wigner, Phys. Rev. **49** (1936) 519.
- [31] Tullio Regge, Nuovo Cim. **14** (1959) 951.
- [32] Stephen Godfrey, Gabriel Karl and Patrick J. O'Donnell, Z. Phys. C **31** (1986) 77.
- [33] A. V. Anisovich and A. V. Sarantsev, Phys. Lett. **B413** (1997) 137 [arXiv:hep-ph/9705401].
- [34] V. V. Anisovich and A. V. Sarantsev, arXiv:hep-ph/0204328.
- [35] Carla Göbel, on behalf of the E791 Collaboration, Proceedings of Heavy Quarks at Fixed Target (HQ2K), Rio de Janeiro, October 2000, 373-384 [hep-ex/0012009]
- [36] Carla Göbel, on behalf of the E791 Collaboration, AIP Conf. Proc. **619** (2002) 63 [arXiv:hep-ex/0110052].
- [37] E. M. Aitala *et al.* [E791 Collaboration], Phys. Rev. Lett. **89** (2002) 121801 [arXiv:hep-ex/0204018].
- [38] Eef van Beveren and George Rupp, AIP Conf. Proc. **619** (2002) 209 [arXiv:hep-ph/0110156].
- [39] Matthias Jamin, José Antonio Oller, and Antonio Pich, Nucl. Phys. **B587**, 331 (2000) [hep-ph/0006045].

- [40] J. A. Oller, E. Oset and J. R. Peláez, Phys. Rev. **D59** (1999) 074001 [Erratum-ibid. **D60** (1999) 099906] [arXiv:hep-ph/9804209].
- [41] V. De Alfaro and T. Regge, *Potential Scattering*, North Holland (Amsterdam, 1965).
- [42] M. Boglione and M. R. Pennington, Phys. Rev. D **65** (2002) 114010 [arXiv:hep-ph/0203149].
- [43] F. De Fazio and M. R. Pennington, Phys. Lett. B **521** (2001) 15 [arXiv:hep-ph/0104289].
- [44] S. N. Cherry and M. R. Pennington, Nucl. Phys. A **688** (2001) 823 [arXiv:hep-ph/0005208].
- [45] W. Lee and D. Weingarten, Phys. Rev. **D61**, 014015 (2000) [hep-lat/9910008]; D. Weingarten, private communication.
- [46] W. Lee and D. Weingarten, Nucl. Phys. Proc. Suppl. **53**, 236 (1997) [hep-lat/9608071].
- [47] Kim Maltman, Phys. Lett. **B462** (1999) 14 [arXiv:hep-ph/9906267].
- [48] Kim Maltman, Nucl. Phys. **A675** (2000) 209c.
- [49] C. M. Shakin, Phys. Rev. D **65** (2002) 114011.